

3  
5  
5  
5

# GMRF MODELS AND WAVELET DECOMPOSITION FOR TEXTURE SEGMENTATION

*Santhana Krishnamachari and Rama Chellappa*

Department of Electrical Engineering and  
Institute for Advanced Computer Studies  
University of Maryland  
College Park, Maryland 20742.

## ABSTRACT

A multichannel scheme for texture segmentation using Gauss Markov random fields (**GMRF**) is presented. We present a family of filters called Markov filters with a property that, when a homogeneous GMRF is filtered with these filters, the resulting output is also a GMRF. We use these filters to decompose images in a fashion similar to the wavelet decomposition, such that the individual subbands are also GMRFs. However, in wavelet decomposition, after filtering, the individual subbands are subsampled and Markov fields lose the Markov property when subsampled. We have shown in [1] that subsampled GMRFs can be efficiently approximated by Markov fields using the *local conditional distribution invariance* approximation. Hence individual subbands can be modeled by GMRFs. We have used this multichannel model to classify remote sensed imagery and to perform texture segmentation.

## 1. INTRODUCTION

Studies on human visual system have revealed the existence of a set of independent channels with specific orientations and spatial frequency tunings [2]. It is believed that the visual system decomposes the retinal image into a number of filtered images. These studies have prompted the development of multichannel models and algorithms for image analysis. Such multichannel schemes rely on decomposing images into different frequency bands and hence enable the frequency specific properties to be analyzed in a greater detail in the individual bands [3], [4], [5], [6]. In this paper, we present a multichannel scheme based on GMRFs for texture segmentation.

## 2. GMRF

Let  $\Omega = \{(i, j) : 0 \leq i \leq M - 1, 0 \leq j \leq N - 1\}$  be a lattice. Let  $\underline{X}$  represent a random vector, obtained by

---

This work was supported in part by Grant #ASC 9318183 from the National Science Foundation

ordering the random variables on the two dimensional lattice  $\Omega$ , through a row-wise scan. The elements of  $\Omega$  are indexed by  $s$ , where  $s = (s_1, s_2)$ . If  $\underline{X}$  is modeled by a GMRF with a symmetric neighborhood  $\eta$ , then  $\underline{X}$  can be written as:

$$X_s = \sum_{r \in \eta} \theta_r X_{s+r} + e_s$$

where  $e_s$  is zero mean, spatially correlated, Gaussian noise with variance  $\sigma^2$ . GMRFs can be completely characterized by the set of parameters  $\{\theta, \sigma^2\}$ .  $\underline{X}$  exhibits the Markov property,

$$\begin{aligned} P(x_s/x_t, \forall t \neq s, t \in \Omega) &= P(x_s/x_{s+r}, r \in \eta) \\ &= \frac{1}{\sqrt{2\pi\sigma^2}} \exp\left\{-\frac{[x_s - \sum_{r \in \eta} \theta_r x_{s+r}]^2}{2\sigma^2}\right\}. \end{aligned}$$

The power spectrum  $S_x$  of  $\underline{X}$  can be shown to be:

$$S_x(\omega_1, \omega_2) = \frac{\sigma^2}{1 - \sum_{r \in \eta} \theta_r \cos\left[\frac{2\pi}{M} r_1 \omega_1 + \frac{2\pi}{N} r_2 \omega_2\right]} \quad (1)$$

$$0 \leq \omega_1 \leq M - 1, 0 \leq \omega_2 \leq N - 1.$$

## 3. IMAGE DECOMPOSITION

Images can be decomposed into different frequency channels by proper selection of frequency selective filters. For an effective analysis of image features in different channels, care must be taken to ensure sufficient spatial localization along with spectral selectivity.

### 3.1. Markov Filters

We use an image decomposition similar to the wavelet decomposition that employs quadrature mirror filters (QMF). The QMF filters were initially used to decompose and code speech signals in subbands. Vetterli [7] extended the 1-D QMF filters to multiple dimensions. The QMF filters in 2-D are denoted by  $h_{11}$ ,  $h_{12}$ ,  $h_{21}$ , and  $h_{22}$  with corresponding Fourier transforms

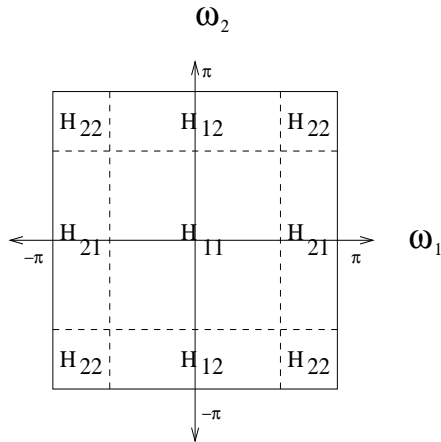


Figure 1:  
Partition of frequency domain

denoted by  $H_{11}$ ,  $H_{12}$ ,  $H_{21}$ , and  $H_{22}$  (Figure 1 shows a typical frequency domain decomposition). The conditions on 2-D QMF filters are :

1. The filters  $H_{11}$ ,  $H_{12}$ ,  $H_{21}$ , and  $H_{22}$  should have the mirror image conjugate symmetry about their mutual boundaries, i.e.,

$$\begin{aligned} H_{12}(w_1, w_2) &= H_{11}(w_1, w_2 + \pi); \\ H_{21}(w_1, w_2) &= H_{11}(w_1 + \pi, w_2); \\ H_{22}(w_1, w_2) &= H_{11}(w_1 + \pi, w_2 + \pi). \end{aligned}$$

2. No aliasing in reconstruction and
3. Perfect reconstruction of the signal from the decomposition.

In our filters, instead of the perfect reconstruction constraint we use a constraint that the filter should be such that, a GMRF on filtering, results in another GMRF. This is acceptable, because in classification and texture segmentation problems, the goal is to decompose the original image into different channels and label each pixel as one of many classes, based on the properties of the pixel in different channels. Hence the perfect reconstruction constraint is not necessary here.

The family of separable, symmetric, linear phase filters that we use for signal decomposition has an amplitude response of the form :

$$|H_1(w)| = \frac{\sqrt{1 - \sum_{i=1}^n \alpha_i}}{\sqrt{1 - \sum_i \alpha_i \cos(iw)}} \quad (2)$$

and

$$|H_2(w)| = |H_1(w + \pi)| = \frac{\sqrt{1 - \sum_{i=1}^n \alpha_i}}{\sqrt{1 - \sum_i (-1)^i \alpha_i \cos(iw)}}$$

The filter is called an  $n$ -th order filter if  $\alpha_i = 0, \forall i > n$ . In all our implementations, we have used first order

filters. The decomposition filters for 2-D are obtained by the separable product,

$$H_{ij}(w_1, w_2) = H_i(w_1)H_j(w_2) \quad i, j = 1, 2.$$

To show that the above filters retain the Markov property of GMRFs, let  $\mathbf{X}$  be a GMRF with parameters  $(\underline{\theta}, \sigma^2)$  and neighborhood  $\eta$ . The power spectral function for the infinite lattice case is given by:

$$S_x(\omega_1, \omega_2) = \frac{\sigma^2}{1 - \sum_{r \in \eta} \theta_r \cos[r_1 \omega_1 + r_2 \omega_2]}$$

and let  $\mathbf{Y}$  be the output resulting from filtering  $\mathbf{X}$  by  $H_{ij}$ . Then,

$$\begin{aligned} y(m, n) &= h_i(m) \odot h_j(n) \odot x(m, n) \\ S_y(\omega_1, \omega_2) &= |H_i(w_1)|^2 |H_j(w_2)|^2 S_x(w_1, w_2) \quad (3) \end{aligned}$$

where  $\odot$  represents convolution. It can be seen that  $S_y$  can be written in a form similar to  $S_x$  with a different set of parameters  $(\tilde{\theta}, \tilde{\sigma}^2)$  and with a larger neighborhood  $\tilde{\eta}$ . Therefore  $\mathbf{Y}$  is also a GMRF. The GMRF parameters of  $\mathbf{Y}$  can be obtained from the parameters of  $\mathbf{X}$  and the filter parameters  $\underline{\alpha}$ . Because of filtering, the neighborhood of the output process is always larger than the neighborhood of the input process. Specifically, with a first order filter, a first order GMRF input results in a fourth order GMRF output and a second order GMRF input results in a fifth order GMRF output.

### 3.2. Markov Approximation

The Markov filters presented in the previous section exhibit the property that a GMRF, when decomposed by these filters, results in another GMRF. However, in wavelet decomposition, the signal representation at a coarser resolution is obtained by filtering and decimating the representation at the immediate higher resolution. Even though the aforementioned filters retain the Markov property on filtering, the subsampling resolution transformation results in the loss of Markov property [8]. We have shown in [1] that subsampled fields can be effectively approximated by GMRFs using the *local conditional distribution invariance approximation*.

Let  $\mathbf{X}$  be the original GMRF and  $\mathbf{Y}$  be the output of filtering  $\mathbf{X}$  by  $H_{ij}$ .  $\mathbf{Y}$  is also a GMRF and the density  $p(\underline{y})$  can be obtained by calculating the parameters from Eq. (3). Let  $\mathbf{Z}$  be the random field obtained by subsampling  $\mathbf{Y}$ . Let  $p(\underline{z})$  be the exact non-Markov density on  $\mathbf{Z}$  and  $q(\underline{z})$  be the family of GMRF densities with a specified neighborhood  $\psi$ . The best GMRF

density  $q^*(\mathbf{z})$  is such that:

$$q^*(z_s/z_{s+r}, r \in \psi) = \arg \min_q D[p(z_s/z_{s+r}, r \in \psi) \parallel q(z_s/z_{s+r}, r \in \psi)],$$

where  $D(\cdot, \|\cdot)$  is the Kullback-Leibler distance. The parameters  $(\underline{\theta}^*, [\sigma^2]^*)$  corresponding to  $q^*(\mathbf{z})$  can be obtained as follows [1]:

$$\begin{aligned} \underline{\theta}^* &= \arg \min_{\underline{\theta}} E_p[Z_s - \sum_{r \in \psi} \phi_r Z_{s+r}]^2 \\ [\sigma^2]^* &= E_p[Z_s - \sum_{r \in \psi} \theta_r^* Z_{s+r}]^2. \end{aligned} \quad (4)$$

#### 4. SEGMENTATION

We use the GMRF based wavelet decomposition to perform segmentation. It is assumed that each lattice site in the image belongs to one of the finite number of label classes, say from  $\{1, 2, \dots, V\}$ . This label field is not directly observable, but an intensity field which statistically depends on the label field is observed. The unobserved label field is estimated from the intensity field.

The label field is modeled by an MRF with a neighborhood  $\psi$ .

$$P(\underline{L} = \underline{l}) = \frac{1}{Z} \exp[\beta \sum_{s \in \Omega} U(l_s)]$$

where  $U(l_s)$  is the number of neighbors in  $\psi$  that have the same label as  $l_s$ . The intensity field is modeled by a GMRF with a neighborhood  $\eta$  and the parameters of this GMRF depend on the label field index at that site. The label field is estimated from the intensity field using the iterated conditional mode (ICM) [9]:

$$\max_{L_s} P(X_s/X_{s+r}, L_s, r \in \eta) P(L_s/L_{s+r}, r \in \psi) \quad (5)$$

##### 4.1. Multichannel Segmentation

###### Algorithm:

1. First, the range of values of the label field is assumed to be finite and known. For each individual value of the label field the corresponding GMRF parameters of the intensity field in the given image are also assumed to be known.
2. The given image is decomposed into four subbands using the Markov filters. The bands are named  $B_{11}$ ,  $B_{12}$ ,  $B_{21}$ , and  $B_{22}$  based on the filter that is used for decomposition. The GMRF parameters corresponding to each label class in each band are obtained by

using Eq. (3) and then Eq. (4). In consequent coarser resolutions the  $B_{11}$  band is decomposed into four subbands.

3. The segmentation is initialized at the coarsest resolution. The  $B_{11}$  band is initially segmented using the ICM algorithm. With the result of segmentation at each lattice site in the  $B_{11}$  band, a confidence measure is attached.

4. The points of low confidence measure are reclassified using the other three bands  $B_{12}$ ,  $B_{21}$ , and  $B_{22}$ . This is done by calculating the sum of the conditional probabilities that a given lattice site belongs to a class in the  $B_{12}$ ,  $B_{21}$ , and  $B_{22}$  bands and the class with the highest probability is chosen.

5. The result of segmentation along with the confidence measures thus obtained is used to initialize the segmentation at the  $B_{11}$  band of the immediate higher resolution and this is repeated until the fine resolution image is classified.

Figure 2 contains grass, calf leather, wool and wood textures. The original GMRF parameters at fine resolution are estimated by a maximum likelihood estimation. Figure 3 shows the single channel ICM segmentation with 14.27% misclassification and Figure 4 shows the multichannel segmentation with 6.0% misclassification. Figure 5 shows a section of multispectral sensor image over Africa. Unfortunately, exact class maps are not available. However, we chose three classes corresponding to river, forest, deforestation. Figure 6 shows the single channel result and Figure 7 shows the multichannel result. It can be observed that the multichannel algorithm has performed better than the single channel algorithm.

#### 5. REFERENCES

- [1] S. Krishnamachari and R. Chellappa, "Multiresolution GMRF models for texture segmentation," *Proc. of IEEE International Conf. on Acoustics, Speech, and Signal Processing*, pp. 2407-2410, May 1995. Also Tech. Rep. CS-TR-3393, University of Maryland, 1995.
- [2] F. W. Campbell and J. G. Robson, "Application of fourier analysis to the visibility of gratings," *J. Physiol., Lond.*, pp. 551-556, 1968.
- [3] J. M. Coggins and A. K. Jain, "A spatial filtering approach to texture analysis," *Pattern Recognition Lett.*, vol. 3, pp. 195-203, 1985.
- [4] A. K. Jain and F. Farrokhnia, "Unsupervised texture segmentation using gabor filters," *Proc.*

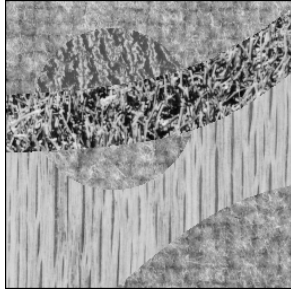


Figure 2:  
Brodatz Textures

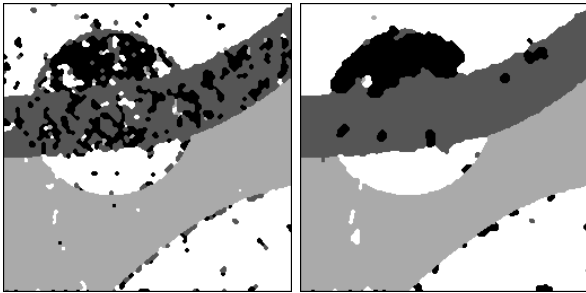


Figure 3:  
Single Channel  
Segmentation

Figure 4:  
Multichannel  
Segmentation

of *IEEE Conf. on Computer Vision and Pattern Recognition*, pp. 364–370, June 1991.

- [5] A. C. Bovik, M. Clark, and W. S. Geisler, “Multichannel texture analysis using localized spatial filters,” *IEEE Trans. Patt. Anal. Mach. Intell.*, vol. 12, pp. 55–73, 1990.
- [6] T. Chang and C. C. J. Kuo, “Texture analysis and classification with tree-structured wavelet transform,” *IEEE Transaction on Image Processing*, vol. 2, pp. 429–442, 1993.
- [7] M. Vetterli, “Multi-dimensional sub-band coding: Some theory and algorithms,” *Signal Processing*, vol. 6, pp. 97–112, Apr. 1984.
- [8] F. C. Jeng, “Subsampling of Markov random fields,” *Jour. of Visual Communication and Image Representation*, vol. 3, pp. 225–229, Sep. 1992.
- [9] J. Besag, “On the statistical analysis of dirty pictures,” *Journal of the Royal Statistical Society*, vol. 48, pp. 259–302, 1986.



Figure 5: Remote Sensed Image

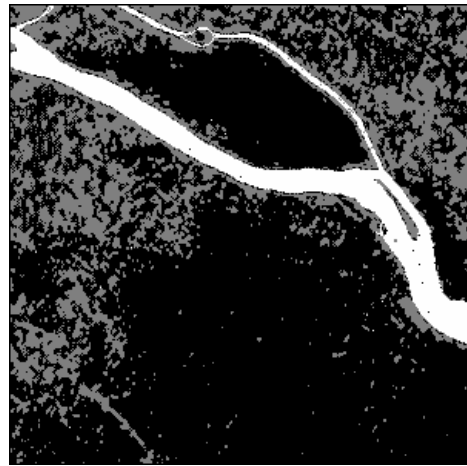


Figure 6: Single Channel Segmentation

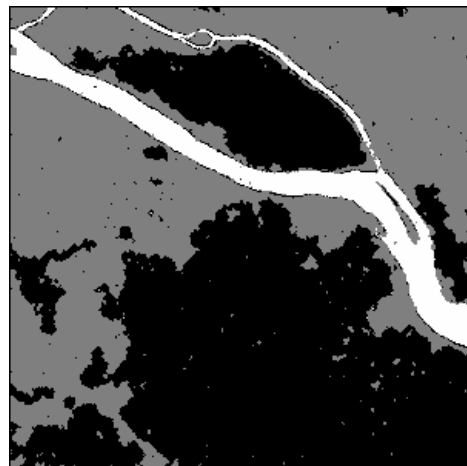


Figure 7: Multichannel Segmentation